PAPER • OPEN ACCESS

Magnetite nanocrystal clusters transformed from ferric precursor and their colloidal magnetorheology

View the article online for updates and enhancements.

IOP | ebooks™

Bringing you innovative digital publishing with leading voices to create your essential collection of books in STEM research.

Start exploring the collection - download the first chapter of every title for free.

Magnetite nanocrystal clusters transformed from ferric precursor and their colloidal magnetorheology

H Abe[1,5], K Kuruma[1], T Murakami[1], M Takahashi[1], K Sato[2], T Naka[3] and Y Suzuki[4]

[1] Joining and Welding Research Institute, Osaka University, 11-1 Mihogaoka, Ibaraki, Osaka 567-0047, Japan;

[2] Graduate School of Science & Technology, Gunma University, 1-5-1 Tenjin-cho, Kiryu, Gunma 376-8515, Japan;

[3] National Institute for Materials Science, 1-2-1 Sengen, Tsukuba, Ibaraki 305-0047, Japan;

[4] Faculty of Pure and Applied Science, University of Tsukuba, 1-1-1 Tennodai, Tsukuba, Ibaraki 305-8573, Japan.

[5] E-mail: h-abe@jwri.osaka-u.ac.jp

Abstract. Spherical magnetite (Fe_3O_4) nanocrystal clusters (MNCs) were synthesized via reductive aging of ferric precursor ($FeCl_3 \cdot 6H_2O$) in ethylene glycol (EG) in the presence of potassium acetate (KOAc). EG was used both as a reducing agent and a solvent. The as-synthesized MNCs with an average diameter of ~500nm comprised Fe_3O_4 nanocrystals with almost equal crystallographic orientation. The time-resolved evolution of the iron species was tracked, and the MNC transformation pathway from the ferric precursor in the solution was deduced. Moreover, to examine the feasibility of MNCs for a field-responsive material, magnetorheology was investigated for the MNC-dispersed colloid.

1. Introduction

Magnetite (Fe_3O_4) is a representative of a large family of ferrites with inverse spinel structure. The controllable synthesis of Fe_3O_4 nanocrystals has excitingly progressed in the past few decades. The focus of synthetic efforts tends to shift toward developing of secondary Fe_3O_4 nanocrystal structures, i.e., Fe_3O_4 nanocrystal clusters, owing to their unique collective properties [1, 2].

Recently, "one-pot" synthesis of spherical Fe_3O_4 nanocrystal clusters (MNCs) without any templates has gained considerable attention [3-8]. Previous synthetic strategies were mostly based on the solvothermal method proposed by Li *et al*. [9]. In this process, MNCs are obtained by the reaction between $FeCl_3 \cdot 6H_2O$ and ethylene glycol (EG), whereas a mild base such as sodium acetate and a surfactant such as polyethylene glycol are added to assist phase and morphological transformations and prevent particle agglomeration. EG is often used as reductive solvent. The reaction temperature is generally 200°C or more for efficient reduction [9-11], which is above its boiling point. However, MNCs formation mechanism and ways to control them are not well understood yet. Particularly, the additives used in this method render the deduction of MNC formation mechanism complicated [12, 13]. Simpler synthetic strategies and protocols may lead to efficient production and elucidation of the formation mechanism.

Herein, we report the simple one-pot process for MNCs, which were produced via the reductive aging of $FeCl_3 \cdot 6H_2O$ in EG only in the presence of potassium acetate (KOAc) as a mild base at $\leq$ 200°C. Owing to the lower reaction temperature, only a glass tube is used as a reaction vessel without using autoclaves. This temperature also enables us to monitor *in situ* color changes during the reaction to successfully determine iron oxide synthesis [14]. This study primarily investigates the effect of water from $FeCl_3 \cdot 6H_2O$ on the MNC transformation pathway. The role of water has not been carefully examined, but recent studies revealed that water is an important additive in this system [15, 16]. Therefore, the time-resolved evolution of iron species is tracked by focusing on the water from the precursor and the MNC transformation pathway is deduced. Moreover, magnetorheology (MR) is explored for an MNC-dispersed colloid as one of the collective properties.

2. Experimental

All chemicals were of analytical grade and used as received without further purification. $FeCl_3 \cdot 6H_2O$ (>99%), anhydrous $FeCl_3$ (>95%), KOAc (>98.5%), and EG (>99.5%) were all purchased from Kishida Chemical Co., Ltd (Osaka, Japan).

For the synthesis of MNCs, two solutions were prepared. One was prepared by dissolving $FeCl_3 \cdot 6H_2O$ in EG (0.2 M) and the other by dissolving KOAc in EG (1.2 M). The two solutions were then mixed with a volume ratio of 1:1 at room temperature, forming yellow precipitate (Figure 1). The yellow colloidal dispersion was transferred into a glass tube (15-mL capacity, Ace Glass Inc.). After reductive aging at 180°C for 24 h in an oil bath, black powder was obtained at the bottom of the tube (Figure 1). Finally, the black product was repeatedly washed with EG and dried in a vacuum oven at 50°C for 6 days. To investigate the effect of water, anhydrous $FeCl_3$ and EG (>99.8%; Sigma-Aldrich) were used instead of $FeCl_3 \cdot 6H_2O$ and EG (>99.5%; Kishida).

For the magnetorheological investigation, a magnetic colloid was prepared from MNCs and silicone oil (KF96-50cs; Shin-Etsu Chemical, Japan). The colloid was homogeneously mixed via ultrasonication (solid concentration ~30 vol%).

The morphologies of the as-synthesized product were observed via field emission scanning electron microscopy (FE-SEM; SU-70; Hitachi High-Tech, Japan). Their phase structures were analyzed via X-ray diffraction (XRD; Multifex, Cu-K_a, 40 kV, and 40 mA; Rigaku, Japan). Transmission electron microscope (TEM), high-resolution TEM (HRTEM) images, and selected area electron diffraction (SAED) patterns were obtained using the JEM 2010F electron microscope (JEOL, Japan). DC magnetization was also measured using a conventional superconducting quantum interference device magnetometer (MPMS-XL; Quantum Design, USA). The MR of the magnetic colloid was measured at room temperature under steady shear flow and static magnetic field using a commercial parallel-plate rheometer (RheoStress 600; Haake, Germany) attached to an electromagnetic system (MR-100N; EKO Instruments, Japan). A magnetic flux was applied perpendicular to the shear flow direction.

Figure 1. Flowchart of the typical synthesis process. Yellow precipitate formed after the mixing process. Black powder was obtained after reductive aging at 180°C for 24 h.

3. Results and discussion

3.1. Structure and morphology of MNCs

The crystalline structure and morphology of the as-synthesized black powder obtained via reductive aging at 180 °C for 24 h were examined. The SEM image (Figure 2a) shows the formation of a large quantity of spheres with an average diameter of ~500nm. In addition, it can be observed from surface of the sphere that they consisted of Fe_3O_4 nanoparticles (Figure 2b). The XRD pattern (Figure 3a) shows that the powder was pure Fe_3O_4 with an inverse spinel structure (ICDD PDF#019-0629). The saturation magnetization of the powder was determined to be 63 emu/g at room temperature. This value is almost the same for MNCs synthesized at 200ºC [4, 10]. We also produced MNCs by the reductive aging at 160 °C for 45 h (not shown here). Thus, it can be said that EG is applicable as a reductive solvent even at below 200 ºC for producing MNCs.

3.2. Formation mechanism of MNCs

To investigate the evolution of iron species, a time-dependent experiment was performed, where MNC formation followed a transformation pathway involving the formation of plate-like intermediates. After reductive aging at 180 ℃ for 6 h, a large amount of plate-like intermediates coexisted with some MNCs with the mean size of ~400 nm (Figure 4a). In their XRD pattern (Figure 3c), an intense peak at $2\theta \approx 8.5°$ is depicted along with some broad weak peaks, besides the Fe_3O_4 phase. These diffraction peaks are similar to that reported for iron alkoxides with a lamellar structure or iron oxide acetate hydroxide hydrate [12, 13]. After the 10 h reaction, the peaks of Fe_3O_4 were strengthened, whereas the other peaks that were considered to be the intermediate phase almost disappeared (Figure 3b). In the corresponding SEM image, MNCs are exclusively observed with a mean size of ~500 nm (Figure 4b). After the 24 h reaction, a slightly better crystalline structure was observed (Figure 3a) whereas the mean size of MNCs remained almost stable.

The growth of MNCs was accomplished by the consumption of the intermediates. Specifically, the phase and morphology of the intermediate and MNC are dissimilar. These different characteristics can be only explained if the reaction proceeds via the solution [17]: the intermediates gradually dissolved and then the precipitation of Fe_3O_4 nanocrystals and MNC enhancement occurred.

The solvent contained water from $FeCl_3$ $6H_2O$ in addition to EG. Further investigation revealed that water plays an important role on the present synthesis. Without water, only the plate-like intermediates were prepared. The mixing of anhydrous $FeCl_3$ and KOAc in EG afforded yellow precipitate (Figure 5a). After aging at 180 ℃ for 2 h, the yellow precipitate settled (Figure 5b) and the plate-like intermediates were observed (Figure 5e). These intermediates were regarded as a ferric compound because the color remained yellowish. Similar intermediates were obtained even after 24 h and their color remained still yellow, indicating that no transformation occurred without water. When water corresponding to the water of $FeCl_3$ $6H_2O$ was added and mixed (Figure 5c), black MNC powder (Figures 5d and 5f) was produced after 180 ℃ for 24 h. Evidently, the intermediates dissolved and MNCs precipitated, triggered by water.
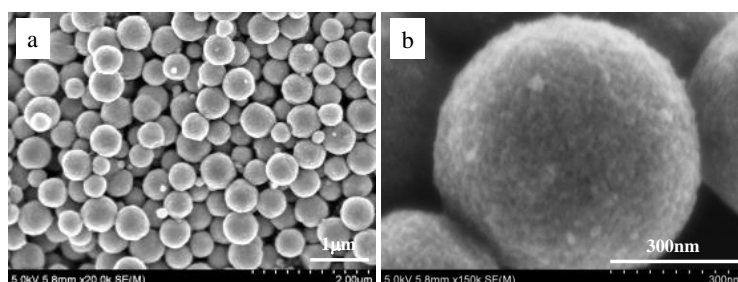

Figure 2. SEM images of as-synthesized MNCs (a) low magnification view, and (b) high magnification view.
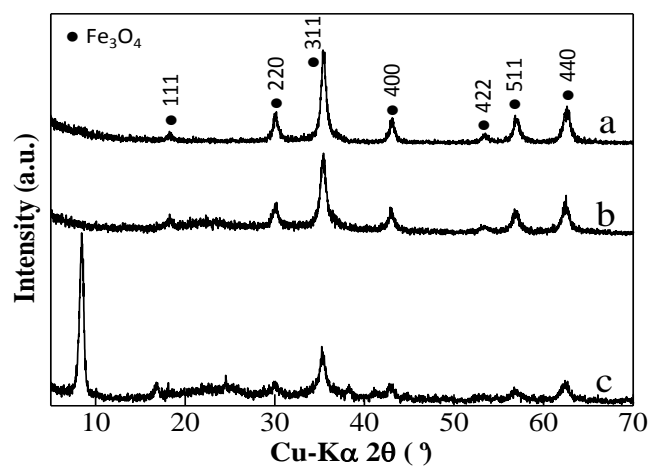
Figure 3. XRD patterns of products obtained via reductive aging at 180°C for (a) 24 h, (b) 10 h and (c) 6 h.
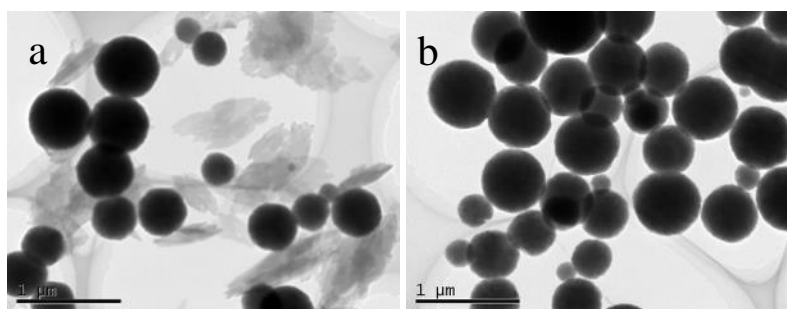

Figure 4. TEM images of products obtained by reductive aging at 180C for (a) 6h and (b) 10h.
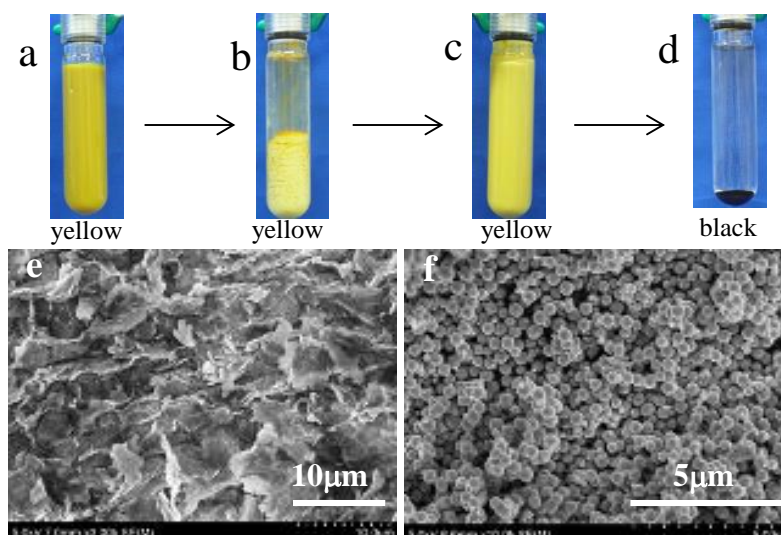

Figure 5. Photos of reaction vessels after **(a)** mixing the anhydrous $FeCl_3$ and KOAc in EG at room temperature, **(b)** aging of the sample (a) at 180°C for 2 h, **(c)** adding water to sample (b) and mixing, and **(d)** reductive aging of the sample (c) at 180 ℃ for 24 h, **(e)** SEM image of sample (b), and **(f)** SEM image of sample (d).
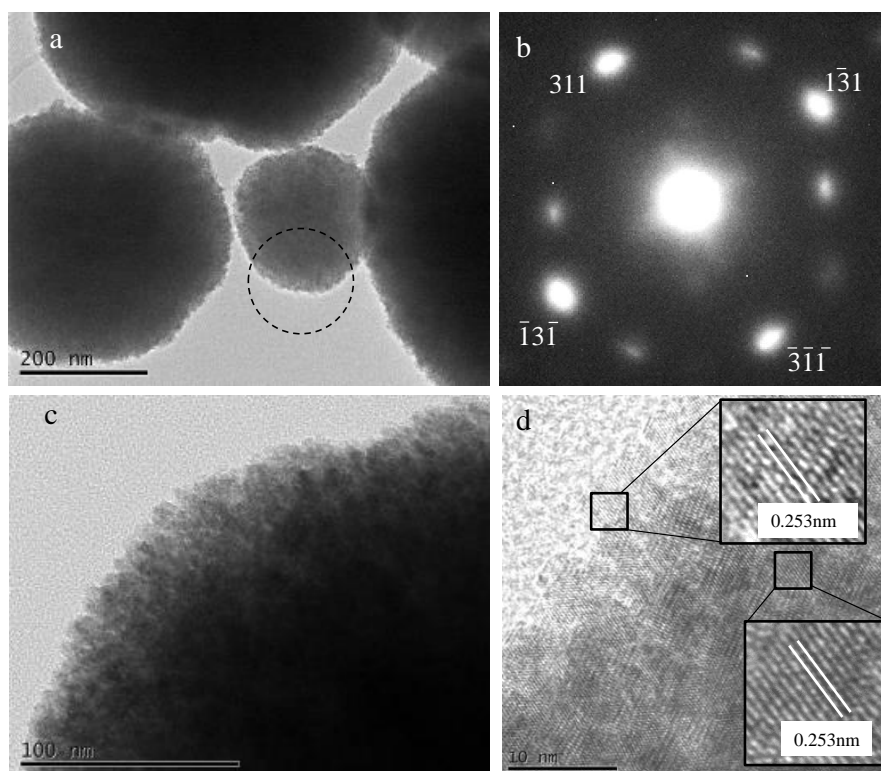
Figure 6. (a) TEM image of MNCs (180 ℃, 10 h). (b) SAED pattern of the circled region in (a). (c) HRTEM image of MNC edge. (d) Magnified HRTEM of (c).

On the basis of above examinations, the formation process of MNC can be summarized. Prior to aging, the yellow precipitates (ferric compounds) were already formed by mixing $FeCl_3$ $6H_2O$ and KOAc in EG. In the early stage of reaction, the yellow plate-like intermediates developed predominantly. Then, these intermediates gradually dissolved, and Fe^{3+} ions were supplied into the solution. Subsequently, EG reduced partially Fe^{3+} to Fe^{2+}, and Fe_3O_4 nanocrystals would be precipitated through the hydrolysis of a mixture of Fe^{3+} and Fe^{2+} ions. Finally, MNCs would develop but not by aggregation of preformed Fe_3O_4 nanocrystals because the nanoparticles generally tend to form loosely branched aggregates. The MNCs might be isotropically grown via the deposition of Fe_3O_4 nanocrystals on the preformed nanocrystal via, e.g., adhesive growth, leading to spherical particles [18].

A crystallographic orientation relation existed among the Fe_3O_4 nanocrystals in MNCs, possibly resulting from the deposition of Fe_3O_4 nanocrystals. Figures 6a and 6b show the TEM image of MNCs (180 ℃, 10 h) and the SAED pattern. The four intense spots in the SAED pattern were indexed from a single crystal along the [2-1-5] zone axis of Fe_3O_4, indicating that MNC is composed of nanocrystals with almost equal crystallographic orientation. The HRTEM image confirms that MNCs are composed of ~5 nm nanocrystals (Figure 6c and 6d). Measuring the distance of two adjacent planes in Figure 6d provides a value of 0.253 nm, corresponding to the lattice spacing of (311) plane of Fe_3O_4. Most Fe_3O_4 nanocrystals are crystallographically aligned with the adjacent ones. This crystal growth mechanism remains in progress and will be reported in the future.

3.3. Magnetorheology of the MNC-dispersed colloid

To examine the feasibility of MNCs for a field-responsive material, MR was investigated for the MNC-dispersed colloid. Figure 7 shows the typical MR response for the MNC-dispersed colloid. In this case, shear stress was measured as a function of the shear rate with three external magnetic flux

densities. Shear stress continuously increases as the magnitude of the flux densities increases. The shear rate dependence of shear stress was almost constant, thereby indicating the Bingham plastic behavior. Extrapolating the shear stress value to zero shear rate can aid in estimating the yield stress. Consequently, the yield stress at B = 0.2 T is ~2.5 kPa, which is ~20 times larger than that of the off-state (B = 0T). When a magnetic field was removed, the MR response was reversibly down to the off-state.

The magnetized MNCs formed robust chain-like structures along the magnetic fields in our case. Generally, the mechanism responsible for the MR effect is the attractive interaction between the induced dipoles, thereby causing the suspended particles to form chain-like structures aligned roughly parallel to the applied magnetic field. A yield stress is developed to achieve these chain-like structures [19]. Because the chain-like structures are attributed to effective interparticle attractions among MNCs, the Brownian motion acting isotropically has a negligible influence on the anisotropic dipole–dipole interaction in the MNC-dispersed colloidal system.

Magnetic colloids with large MR effect have elicited scientific and practical interest [20, 21]. Although a ferrofluid is a popular magnetic colloid, it has very low MR effect [19, 22] because superparamagnetic Fe_3O_4 nanoparticles used in the ferrofluid are too small to induce interparticle attraction necessary in forming chain-like structures under the Brownian motion. Moreover, increasing the size enhances the saturation magnetization. However, this process induces the superparamagnetic–ferromagnetic transition (at a domain size of r_c ~ 30 nm for Fe_3O_4 [10]) to ensure that the nanocrystals are no longer dispersible in the solvent.

Meanwhile, the MNCs comprising the nanocrystals formed a robust chain-like structure. In addition, they may be expected to retain the superparamagnetic characteristics because the nanocrystal sizes in MNCs are smaller than the critical value of r_c [10]. If magnetic colloidal particles with high magnetization and superparamagnetic characteristics are available, then these particles may have a potential to be used as magnetic field-responsive materials.
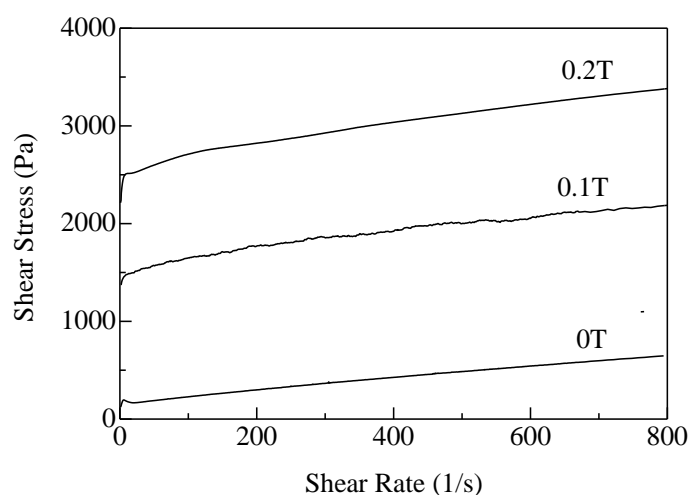
Figure 7. Shear stress as a function of shear rate for MNC-dispersed colloid with magnetic flux densities of 0, 0.1, and 0.2 T.

4. Conclusions

MNCs were successfully synthesized via reductive aging of $FeCl_3 \cdot 6H_2O$ in EG in the presence of KOAc at a reaction temperature lower than that reported in previous studies, thus enabling the utilization of a glass tube as the reaction vessel. Hence, scale up can be easy because no autoclaves were required. This reaction offers an excellent system to understand the MNC transformation in the EG–water mixed solvent owing to its simplicity and to monitor the *in situ* color changes. By

performing a time-resolved experiment focusing on water from $FeCl_3 \cdot 6H_2O$, the result showed that the plate-like intermediates developed from yellow precipitates owing to the mixture of $FeCl_3 \cdot 6H_2O$ and KOAc in EG. Then, the intermediates dissolved gradually, and Fe^{3+} ions were supplied into the solution. Subsequently, EG reduced partially from Fe^{3+} to Fe^{2+}, and Fe_3O_4 nanocrystals would be precipitated through the hydrolysis of a mixture of Fe^{3+} and Fe^{2+} ions. MNCs might be isotropically grown via deposition of Fe_3O_4 nanocrystals on the preformed nanocrystal. MR was also explored for the MNC-dispersed colloid.

Acknowledgments

References

[1]   Liu S, Lu F, Jia X, Cheng F, Jiang L, Zhu J 2011 *CrystEngComm* **13** 2425
[2]   Ge J, Hu Y, Yin Y 2007 *Angew. Chem.* **119** 7572
[3]   Jia B, Gao L 2008 *J. Phys. Chem. C* **112** 666
[4]   Xuan S, Wang Y, Yu J, Leung K 2009 *Chem. Mater.* **21** 5079
[5]   Cheng C, Wen Y, Xu X, Gu H 2009 *J. Mater. Chem.* **18** 8782
[6]   Cheng W, Tang K, Qi Y, Sheng J, Liu Z 2010 *J. Mater. Chem.* **20** 1799
[7]   Sun Q, Ren Z, Wang R, Chen W, Chen C 2011 *J. Nanopart. Res.* **12** 213
[8]   Gao J, Ran X, Shi C, Cheng H, Cheng T, Su Y, 2013 *Nanoscale* **5** 7013
[9]   Deng H, Li X, Peng Q, Wang X, Chen J, Li Y 2005 *Angew. Chem.* **117** 2842
[10]   Ge J, Hu Y, Biasini M, Beyermann W Yin Y 2007 *Angew. Chem.Int. Ed.* **46** 4342
[11]   Wang X, Yu J, Shi G, Xu G, Zhang Z 2014 *J. Mater. Sci.* **49** 6029
[12]   Fan T, Pan D, Zhang H 2011 *Ind. Eng. Chem. Res.* **50** 9009
[13]   Wan J, Tang J, Zhang C, Yuan R, Chen K 2015 *ChemComm* **51** 15910
[14]   Schwertmann U, Cornell R 2000 *Iron Oxides in the Laboratory* (Wiley-VCH)
[15]   Zhang D, Lu C, Ni Y, Xu Z, Zhang W 2013 *CrystEngComm* **15** 4755
[16]   Tong G, Liu Y, Wu T, Tong C, Du F 2015 *J. Mater. Chem.* **3** 5506
[17]   Fievet F, Lagier J, Blin B, Beaudoin B, Figlarz M 1989 *Solid State Ionics* **32/33** 198
[18]   Sunagawa I 1999 *Forma* **14** 147
[19]   Carlson J, Jolly M 2000 *Mechatronics* **10** 555
[20]   Yamanaka S, Abe H, Naito M, Fujimoto T, Kuga Y 2012 *Colloids and Surface A* **415** 239
[21]   Noma J, Abe H, Kikuchi T, Furusho J, Naito M 2010 *J. Mag. Mag. Mater.* **322** 1868
[22]   Lemaire E, Meunier A, Bossis G, Liu J, Felt D, Bashtovoi P, Matoussevitch N 1995 *J. Rheol.* **39** 1011